Analyst

ROYAL SOCIETY OF CHEMISTRY

PAPER

View Article Online
View Journal | View Issue

Check for updates

Cite this: *Analyst*, 2022, **147**, 4500

Ion-selective membrane modified microfluidic paper-based solution sampling substrates for potentiometric heavy metal detection†

Rochelle Silva,[a,b] Ke Zhao,[b,c] Ruiyu Ding,[b,c] Wei Ping Chan,[b] Mingpeng Yang,[b,d] Jane Si Qi Yip[c] and Grzegorz Lisak *[b,c]

Received 10th July 2022,
Accepted 14th August 2022

DOI: 10.1039/d2an01108e

rsc.li/analyst

Paper-based microfluidic solution sampling is a viable option for potentiometric sensors to be used for the determination of analytes in samples with high solid-to-liquid ratios. Unfortunately, heavy metal sensitive electrodes cannot be easily integrated with paper-based solution sampling as heavy metals have strong physicochemical adsorption affinity towards paper substrates. In this work, paper substrates were modified with an ion-selective membrane (ISM) cocktail (used for the preparation of Pb^{2+}-ion-selective electrodes (ISEs)) and coupled with model heavy metal Pb^{2+}-ISEs. It was found that the super-Nernstian response of Pb^{2+}-ISEs was eliminated when 10 to 50 mg ml^{-1} of the ISM cocktail was used for the modification of paper substrates. The modification of the paper substrates by Pb^{2+}-ISM allowed the elimination of adsorption sites. In addition, it resulted in an improvement of sensor performance in terms of their detection limits to be similar to those for conditioned electrodes in standard beaker-based measurements. It is believed that the elimination of super-Nernstian response of the electrodes and improving the potentiometric responses and detection limits of ISEs were attributed to the compatibility improvement of the paper substrates and Pb^{2+}-ISEs to the same type of ISM.

Published on 17 August 2022. Downloaded on 28/1/2026 8:06:14 PM.

Introduction

Potentiometric ion-selective electrodes (ISEs) equipped with polymeric membranes are widely used to measure a variety of ions in clinical and environmental samples.[1–4] Their low cost, versatility, and low power consumption make them more desirable in affordable analytical solutions compared to other standard analytical techniques such as atomic absorption, cold vapour atomic fluorescence, and inductively coupled plasma (mass or optical discrimination).[5–9] Recently, the applications of ISEs have been enhanced by the conversion of electric potential in an ISE into other optical[10,11] or electrochemical[12,13] signals to improve sensitivity.[14]

The use of microfluidic paper-based substrates for solution sampling rather than the traditional beaker-based measurements adds advantages to the analytical protocol of specific sample types, *e.g.* it requires only a small sample volume and allows analysis of samples consisting of high solid-to-liquid ratios.[15–20] However, the use of paper-based microfluidic solution sampling coupled with potentiometric sensors poses some challenges when the target analytes are heavy metals.[21,22] The interactions of heavy metal ions with negatively charged groups commonly present in cellulose cause a deviation from the usual Nernstian response of the ISEs.[23] For example, in the case of Pb^{2+}-ISEs, the thermodynamically expected Nernstian response ought to be 29.6 mV dec^{-1}. Even though a deviation of about ±2 mV is acceptable due to unideal measuring conditions, Pb^{2+}-ISEs coupled with unmodified paper-based substrates show inconsistent slopes along the calibration curve which also are considerably higher and are thus termed "super-Nernstian". This effect is particularly observed between $10^{-3.1}$ and $10^{-4.0}$ mol dm^{-3} $Pb(NO_3)_2$.[23] This observation provides a simple way to determine the efficacy of a paper substrate modification aimed at controlling the physicochemical interactions of heavy metal ions with paper; the linearity of the calibration curve obtained from an electrode coupled with a modified paper substrate, ideally in a wide concentration range, allows it to be used conveniently for analysis of samples with unknown concentrations. Several modifications to the paper-based substrates have been

[a]*Interdisciplinary Graduate Programme, Nanyang Technological University, 61 Nanyang Drive, Academic Block North, Singapore 637335, Singapore*
[b]*Nanyang Environment and Water Research Institute, Residues and Resource Reclamation Center, 1 Cleantech Loop, Cleantech, Singapore, 637141, Singapore. E-mail: g.lisak@ntu.edu.sg*
[c]*College of Engineering, School of Civil and Environmental Engineering, Nanyang Technological University, 50 Nanyang Avenue, Singapore, 639798, Singapore*
[d]*School of Automation, Nanjing University of Information Science and Technology, Nanjing 210044, China*
† Electronic supplementary information (ESI) available. See DOI: https://doi.org/10.1039/d2an01108e

This journal is © The Royal Society of Chemistry 2022

Published on 17 August 2022. Downloaded on 28/1/2026 8:06:14 PM.

explored for the purpose of eliminating or controlling the super-Nernstian response of ISEs. These include the modification of paper with inorganic salts,[24] acid treatment,[25] or creating a physical barrier on the paper substrates (sputtered metal).[26] These techniques either deplete the active sites on the paper substrates or prevent the heavy metal ions from reaching active sites.

The ion-selective membrane (ISM) in an ISE is a vital part that enables the electrode to identify and quantify the target ions in the samples. An ISM typically consists of an ionophore,[1] an ionic additive,[27] a plasticizer,[28] and a polymer matrix.[29] Typically, organic lipophilic substances which can selectively bind to the target ion are used as ionophores and these constitute about 0.5–2% of the dry mass of membrane components. The bulk of the dry mass is usually composed of the polymer matrix mixed with the plasticizer. Such a matrix adds elasticity to the membrane, provides more homogeneous redistribution of the membrane components and enhances ion transport within an ISM.[30] The ionic additives further enhance the ISE's Nernstian behaviour.[27] When the ISE is in contact with the sample solution, the target ions will reach an electrochemical equilibrium at the sample|ISM interface. The potential established at this interface theoretically is proportional to the activity of the ion in the solution, providing a base for an analytical determination of an analyte in the sample with an unknown concentration of the primary ion.[31]

Modifying paper substrates with the ISM components could possibly change the sample|ISM interface and alter/improve the potentiometric response of the electrode eliminating the super-Nernstian behaviour of ISEs that is observed when heavy metal sensitive ISEs are coupled with unmodified paper substrates. This study investigates the effect of modifying paper substrates with different combinations of ISE's membrane components and using them for the solution sampling purpose coupled with Pb^{2+}-ISEs. A favorable combination of membrane components for paper substrate modification was identified.

Experimental

Preparation of ion-selective electrodes and microfluidic paper-based solution sampling substrates

All information about chemicals, materials and electrodes is provided in the ESI (section 1.1).† Glassy carbon (GC) electrodes were polished on a soft mesh using 0.3 μm alumina slurry and subjected to rinsing with ultra-pure water. Electropolymerization on GC was performed by applying a constant current of 0.014 mA (0.2 mA cm^{-2}) for 714 s (ref. 32) in a three-electrode cell using a Gamry interface 1000 potentiostat (Gamry, USA). The electropolymerization solution consisted of 0.01 M EDOT and 0.1 M NaPSS. A platinum mesh was used as the counter electrode and Ag/AgCl (3 M KCl) served as the reference electrode. Afterwards, electrodes were rinsed with ultra-pure water and left to dry overnight at room temperature (23 ± 2 °C). A Pb^{2+} selective membrane cocktail was prepared by mixing 1% lead ionophore IV, 0.5% KTClPB, 65.2% *o*-NPOE and 33.3% PVC (with a total dry mass of 100 mg) in 2 ml of THF and stirred until complete dissolution for 2 h. For the membrane drop-casting, three portions of 20 μL of membrane cocktail were cast on top of the GC/PEDOT electrode with a 1 hour interval between doses. After the final dose, the electrodes were left overnight at room temperature for evaporation of the residual solvent and transferred to 10^{-3} M $Pb(NO_3)_2$ for 24 h of conditioning. The same conditioning solution was used for storage of electrodes in between measurements.

Preparation of paper substrates was carried out by first soaking the filter paper in ultra-pure water for 30 min with gentle stirring followed by oven drying at 70 °C for 30 min. Paper substrates were then cut into 2 × 2 cm^2 pieces. Unmodified paper substrates were referred to as PS0. Modified paper substrates were obtained by soaking the washed and dried pieces of paper substrates in the respective solutions for 30 min with gentle stirring followed by drying at room temperature overnight (Table S1 in the ESI†).

Furthermore, different dilutions of PS6.0 were also studied, and the paper substrates were named PS6.1, PS6.2, PS6.3, PS6.4, PS6.5, and PS6.6, with membrane cocktail concentrations of 35, 25, 10, 5, 1, and 0.1 mg of total dry mass in 1 ml of THF, respectively. For ease of reference, it is to be noted that 50 mg ml^{-1} is the standard concentration of ISM used for the preparation of Pb^{2+}-ISEs in this work.

Potentiometric measurements with Pb^{2+}-ISEs

Potentiometric measurements were carried out using an EMF16 Interface potentiometer, Lawson Labs Inc. For both beaker-based and paper-based measurements, the response of Pb^{2+}-ISEs in lead(II) nitrate solutions ranging from $10^{-7.0}$ to $10^{-1.4}$ M in ion activity was logged in ascending order of primary ion activity. The Debye–Hückel approximation was used for the calculation of activity coefficients.[33] Ag/AgCl (3 M KCl) was used as the reference electrode. For each indicator electrode, the EMF was logged for 60 s with a data acquisition interval of 1.3 s. Three consecutive measurements were taken at each ion activity for each electrode to calculate uncertainty in the form of standard deviation (n = 3). The response time of electrodes was determined by identifying the times at which the EMF reading of ISEs became stable (n = 3). Standard deviations in figures and text indicate measurement-to-measurement repeatability for an electrode unless stated otherwise.

Traditional beaker-based measurements were performed first to identify the electrodes which showed Nernstian response of Pb^{2+}-ISEs, *i.e.*, a slope of 29.6 ± 2 mV dec^{-1}. Those electrodes were then paired with paper-based microfluidic solution sampling substrates which had been previously prepared. The standard or sample solutions were pipetted onto the paper substrates according to the maximum holding capacity of the substrates. Then the indicator and reference electrodes supported onto a laboratory stand were placed on top of the paper substrates. Initially, the potentiometric responses with paper substrates modified with different combinations of membrane components were studied followed by

Published on 17 August 2022. Downloaded on 28/1/2026 8:06:14 PM.

the response with paper substrates modified with different concentrations of ISM. The detailed information about the experiments based on modified measurement conditions is provided in the ESI (section 1.3).†

The selectivity coefficients for Pb^{2+} over eight interfering ions were obtained using the separate solution method (SSM).[34] The ion sequence was estimated from the literature available on the selectivity of lead ionophore IV[35,36] and confirmed using beaker-based measurements prior to measurements with paper-based substrates. The slopes of Pb^{2+}-ISEs between $10^{-3.06}$ and $10^{-2.17}$ M Pb^{2+} were ensured to be close to Nernstian (namely, for Pb^{2+}-ISEs in beaker based measurements: 28.3 ± 0.2 and for Pb^{2+}-ISEs coupled with PS6.0: 27.5 ± 1.8) and used for calculation of selectivity along with potentials recorded in solutions of interfering ions. The uncertainty of selectivity coefficients was calculated by recording the EMF generated with three electrodes (n = 3).

Characterization of modified paper substrates was also done, and the detailed information is provided in the ESI (section 1.4).† Different environmental samples, including chemical spill, cultivation soil, wetland, and biowaste samples subjected to Toxicity Characteristic Leaching Procedure (TCLP) metal leaching procedure,[37] were used to validate the sensor performance. The detailed information about the samples and the determination of Pb^{2+} is provided in the ESI (section 1.5).†

Results and discussion

Paper-based microfluidic solution sampling using ISM-component modified paper substrates coupled with Pb^{2+}-ISEs

Several physical and chemical modifications of paper-based substrates have been investigated previously to diminish or control the super-Nernstian responses which occur during the detection of heavy metals with cellulose-based paper substrates coupled with potentiometric sensors. For example, pretreatment of the paper substrates with an inorganic salt of the respective primary cation was found to be effective for the detection of Pb^{2+} and Cd^{2+} ions.[24] For Pb^{2+}-ISEs, using filter paper treated with 10^{-3} M $Pb(NO_3)_2$ and then drying prior to solution sampling resulted in a Nernstian response in the range of $10^{-5.0}$ to $10^{-2.17}$ M $Pb(NO_3)_2$. Acidification of paper substrates[25] and sputtering both sides of paper substrates with metal[26] were also found to be effective for Pb^{2+} ion detection. In the case of paper acidification,[25] the optimum potentiometric response was obtained when Pb^{2+}-ISEs were coupled with paper substrates (containing the sample solution) at a pH range of 3 to 4. A linear response could be obtained in the range of $10^{-5.0}$ to $10^{-2.17}$ M $Pb(NO_3)_2$ with a lower detection limit of 10^{-5} M Pb^{2+}. The potentiometric response obtained with metal modified paper substrates[26] was found to be dependent on the thickness and type of the metal used, and the optimum response was obtained with paper substrates coated with gold of 38 nm thickness on both sides. It showed a linear response of 31.3 ± 1.4 mV dec^{-1} in the range of $10^{-5.0}$ to $10^{-2.2}$ M $Pb(NO_3)_2$. One of the disadvantages of these methodologies is that the pretreatment of paper substrates requires additional chemicals apart from the ones used in the preparation of the ISE. Moreover, the physicochemical nature of the ISM|modified paper substrate interface is vastly changing depending on the modification of the paper substrate applied. This in turn may introduce additional interferences to the potential formation at the ISM, simply originating from the proximity of the ISM to the modified paper substrates. The use of the ISM components which are already used in the ISM preparation can simplify the preparation protocol of the modified paper substrates by requiring less chemicals to be used but also simplify the ISM|modified paper substrate interface by being more compatible with the one of ISM. Thus, the modifications of paper substrates with ISM components were studied with the objective of controlling the super-Nernstian responses which occur when Pb^{2+}-ISEs are coupled with cellulose-based paper substrates.

First, paper substrates were modified with single ISM components as mentioned in Table S1.† As shown in Fig. 1, most paper substrates showed a super-Nernstian response which was observed between $10^{-3.06}$ and $10^{-4.02}$ M Pb^{2+}, similar to the response on unmodified paper substrates (PS0). In the case of PS1.0 (PVC and THF) and PS2.0 (PVC, *o*-NPOE and THF), even though the super-Nernstian jump was not observed between $10^{-3.06}$ and $10^{-4.02}$ M, the initial slope of the Pb^{2+}-ISEs was sub-Nernstian between $10^{-3.06}$ and $10^{-2.17}$ M Pb $(NO_3)_2$ (22.8 ± 1.8 mV dec^{-1} for PS1.0 and 20.0 ± 7.0 mV dec^{-1} for PS2.0), limiting the Nernstian response of the Pb^{2+}-ISEs to a very narrow activity range with a lower detection limit of about $10^{-4.0}$ M Pb^{2+}. PS3 (o-NPOE and THF) and PS5.0 (lead ionophore IV and THF) had super-Nernstian jumps of 51.6 ± 4.7 mV dec^{-1} and 80.0 ± 8.0 mV dec^{-1} between $10^{-3.06}$ and $10^{-4.02}$ M Pb^{2+}, respectively. PS4.0 (KTClPB and THF) seemingly showed high uncertainty at each ion activity which was

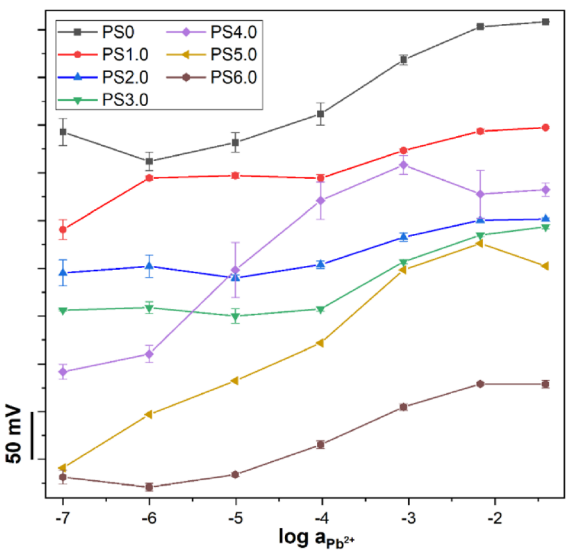

Fig. 1 Potentiometric response of Pb^{2+}-ISEs coupled with ISM-component modified paper substrates.

This journal is © The Royal Society of Chemistry 2022

Published on 17 August 2022. Downloaded on 28/1/2026 8:06:14 PM.

found to be too high to be considered experimentally useful. However, the increase of the initial Nernstian slope of PS2.0 (PVC, *o*-NPOE and THF) between $10^{-3.06}$ and $10^{-2.17}$ M $Pb(NO_3)_2$ was obtained by additionally adding to the paper substrate modifying solution other typical membrane components, such as KTClPB and lead ionophore IV. In this case, all ISM-component modified paper substrates PS6.0 (lead ionophore IV, KTClPB, PVC, *o*-NPOE and THF) coupled with Pb^{2+}-ISEs resulted in a favourable potentiometric response with a close to Nernstian linear slope of 34.9 ± 3.3 mV dec^{-1} in the range of $10^{-5.0}$ to $10^{-2.17}$ M $Pb(NO_3)_2$, and the lower detection limit of $10^{-5.4}$ M Pb^{2+}. This could be obtained since the exact composition of the electrode's ISM was used to modify the paper substrate allowing to chemically simplify the paper substrate|Pb^{2+}-ISE interface, thus increasing the compatibility of the paper substrate to the ISM of the Pb^{2+}-ISEs.

Since PS6.0 performed the best out of the investigated paper substrates, variations of PS6.0 were prepared by changing the concentration of the membrane cocktail components in THF that were used for manufacturing the modified paper substrates. This was performed in order to determine whether the Nernstian response of the Pb^{2+}-ISEs could be obtained when coupled with paper substrates modified with membrane cocktail concentrations lower than the usual concentration used in the ISM preparation (50 mg ml^{-1} dry mass of ISM components in THF). This could be beneficial for reducing the amount of chemicals used for the modification of paper substrates. According to Fig. 2, paper substrates 6.6 to 6.4 (0.1, 1, and 5 mg ml^{-1} dry mass of ISM components in THF) showed either super-Nernstian responses or random potential responses which were not conducive to the potentiometric determination of Pb^{2+} ions. This could be because the concentration of ISM components on the paper substrates was not sufficient to modify the surface and the bulk of the paper substrates. A favorable potentiometric response could be obtained for paper substrates 6.3 to 6.0 (10, 25, 35, and 50 mg ml^{-1} dry mass of ISM components in THF). PS6.3 had a slope of 30.8 ± 1.7 mV dec^{-1} in the range of $10^{-4.0}$ to $10^{-2.2}$ M $Pb(NO_3)_2$ and PS6.2 had a slope of 25.8 ± 0.5 mV dec^{-1} in the range of $10^{-6.0}$ to $10^{-2.2}$ M $Pb(NO_3)_2$. The slope for PS6.1 was 29.6 ± 1.3 mV dec^{-1} between $10^{-4.0}$ and $10^{-2.2}$ M $Pb(NO_3)_2$, and for PS6.0 it was 34.9 ± 3.3 mV dec^{-1} in the range of $10^{-5.0}$ to $10^{-2.2}$ M $Pb(NO_3)_2$. Even though the lower detection limit varied between $10^{-6.0}$ and $10^{-4.0}$ M $Pb(NO_3)_2$, Nernstian responses of Pb^{2+}-ISEs could be observed for a sufficient concentration range that would allow target analysis in specific sample types.

Effect of different measurement configurations on the potential formation at the paper substrate|ISM interface

As shown in Fig. 3, PS6.0 was used in different potentiometric measurement configurations to see the effect of different measurement configurations on the potential formation at the paper substrate|ISM interface. The same electrode was used for all measurements to avoid challenges related to the reproducibility of the measurements done by a set of different electrodes. It could be observed that the potentiometric responses of Pb^{2+}-ISE were dependent on the measuring setup investigated. It was reported previously that slopes of ISEs when used with microfluidic paper-based sampling were in general higher than for the same electrodes in beaker-based measurements.[23] Similarly here, the slope of the Pb^{2+}-ISE for microfluidic paper-based solution sampling was 30.7 ± 0.7 mV dec^{-1} in the range of $10^{-5.0}$ and $10^{-2.2}$ M in comparison with the same electrode in beaker-based measurements with a slope of 27.2 ± 0.9 in the range of $10^{-5.0}$ and $10^{-2.17}$ M Pb^{2+}. Interestingly, when the same electrode was placed on the paper substrate that was immersed in the solution, the potentiometric response of the Pb^{2+}-ISE was characterized with a higher than Nernstian response of 35.8 ± 1.7 mV dec^{-1} in the range of $10^{-5.0}$ to $10^{-2.2}$ M Pb^{2+}. This shows that the presence of a

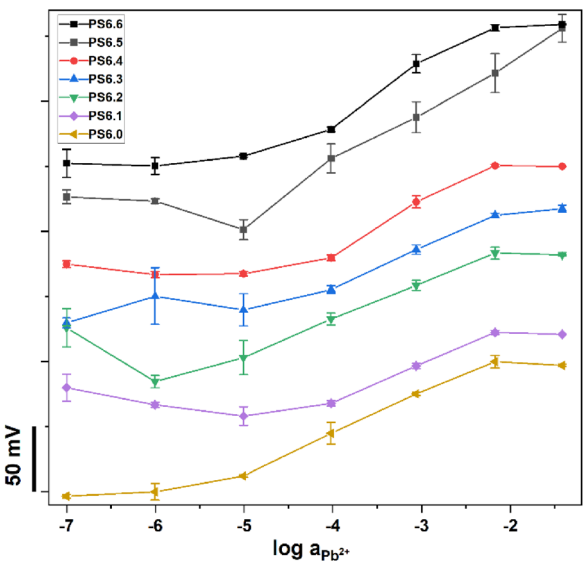

Fig. 2 Potentiometric response of Pb^{2+}-ISEs coupled with paper substrates modified with different concentrations of Pb^{2+} membrane cocktail.

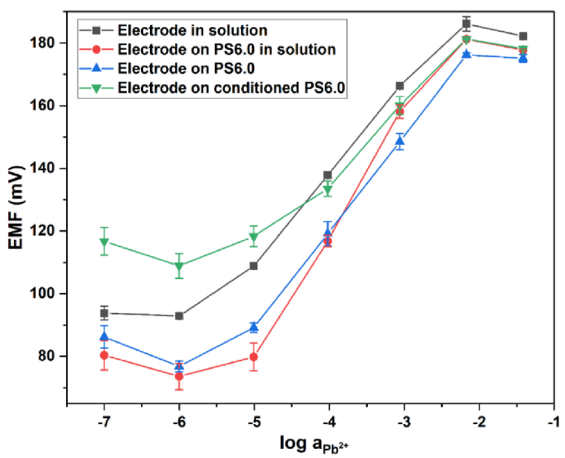

Fig. 3 Potentiometric response of Pb^{2+}-ISEs in different measurement configurations when coupled with PS6.0.

Published on 17 August 2022. Downloaded on 28/1/2026 8:06:14 PM.

larger volume of solution around the electrode that is available for the paper substrate does not necessarily improve the potentiometric response of the electrode. The physicochemical state of the paper substrate that is in direct contact with the ISM during the microfluidic paper-based solution sampling drives the potentiometric response of the Pb^{2+}-ISE. This is valid despite the general availability of the sample solution to the electrode, which was vastly higher than the sorption capacity of the paper substrates. Thus, in this case, a local equilibrium between the ISM and the paper substrate was established driven by the paper substrate's physical and chemical interactions with the sample solution and electrode. Finally, the potentiometric measurements done on paper substrates that were conditioned with primary ions resulted in the formation of slopes comparable to that of beaker-based measurements (25.9 ± 1.3 mV dec^{-1}) but with a much higher detection limit of $10^{-4.0}$ M Pb^{2+}. In theory, a longer contact time for the sample solution should lead to better absorption of the ions on the paper substrate. However, experimentally, this has resulted in a reduction in the linear range of the calibration curve of Pb^{2+}-ISE. This implies that additional conditioning with the sample solution also does not improve the potentiometric response with PS6.0, as possible over-conditioning of the paper was done which could result in possible desorption of the ion (Pb^{2+}) from the paper substrate to the sample solution when in contact with low concentrations of Pb^{2+}. Similar observations were made for other modifications of the paper substrates.[24]

Since modification of the paper substrate with ISM resembles common practice in the preparation of all-integrated paper-based ISEs,[15,38–40] the measurement configuration of using PS6.0 with electrodes which only had PEDOT (PSS) (without Pb^{2+}-ISM) was also explored to see if the ISM on the ISE could be disposed of to simplify the setup to the ones reported for all-integrated paper-based ISEs.[15,38–40] PS6.0 was used in both unconditioned and conditioned (conditioned in 10^{-3} M Pb^{2+} solution for 24 hours, washed with water and then dried) states. As shown in Fig. S2,† the electrode coupled with unconditioned PS6.0 displayed a linear response of 27.2 ± 3.8 mV dec^{-1} in the range of 10^{-5} to $10^{-2.17}$ M Pb^{2+}. For the electrode coupled with conditioned PS6.0, a linear response of 14.0 ± 3.8 mV dec^{-1} was observed in the range of 10^{-4} to $10^{-2.17}$ M Pb^{2+}. Thus it can be concluded that the conditioning state of the ISM and PS6.0 plays an important role in potential formation and stability at the PS6.0|PEDOT(PSS) based electrode interface. The conditioned PS6.0 may be saturated with salt within the available paper matrix and the ISM, affecting the sample concentration and solution availability in the subsequent solution sampling. It is believed that the ionic and water conditions are different at the PS6.0|PEDOT(PSS) based electrode interface for the two cases presented. Moreover, in both cases, the EMF values had higher uncertainty in the lower activity of Pb^{2+} (*e.g.* at 10^{-4} M Pb^{2+}, for unconditioned and conditioned PS6.0, the values were 7.6 and 12.9 mV, respectively) than the ones reported for Pb^{2+}-ISEs (3.8 mV). Although the PEDOT(PSS) based electrode could potentially be used when coupled with unconditioned PS6.0 for specific measurement conditions, the overall sensitivity of the PEDOT (PSS) based electrode to the conditioning state of the paper substrate and higher uncertainties of potential response highlight the importance of a well-conditioned ISM on the PEDOT (PSS) based electrode for a good potentiometric performance with PS6.0 towards Pb^{2+} detection.

Effect of conditioning the ISM modified paper substrates with primary (Pb^{2+}) and interfering ions on the potential formation at the Pb^{2+}-ISEs coupled with microfluidic paper-based solution sampling

The effect of conditioning the ISM modified paper substrates with $Pb(NO_3)_2$ (primary ion) was studied to identify if it can further improve the potentiometric performance of the Pb^{2+}-ISEs coupled with microfluidic paper-based solution sampling (Fig. 4A). Fig. 4B further illustrates how the EMF varied at different Pb^{2+} activities for Pb^{2+}-ISEs coupled with ISM-component modified paper substrates conditioned with different activities of Pb^{2+}. The potentiometric response was logged only for a limited concentration range at which a super-Nernstian response of Pb^{2+}-ISEs could be usually observed. When considering the average slope of potentiometric response between $10^{-2.2}$ M and $10^{-4.0}$ M Pb^{2+}, there was a gradual increase in the slope for PS6.0 conditioned with $10^{-1.42}$ M to $10^{-6.00}$ M Pb^{2+} solutions. The slopes were 19.8 ± 0.7, 22.1 ± 2.2, 25.0 ± 1.5, 25.8 ± 2.3, 27.1 ± 2.5, and 28.3 ± 2.0 mV dec^{-1}, for PS6.0 treated with $10^{-1.42}$, $10^{-2.17}$, $10^{-3.06}$, $10^{-4.02}$, $10^{-5.01}$, and $10^{-6.00}$ M Pb^{2+}, respectively. In comparison, the slope of the unconditioned PS 6.0 was 29.4 ± 1.1 mV dec^{-1}. Also, the EMF that was recorded during different Pb^{2+} activities for Pb^{2+}-ISEs was coupled with ISM component modified paper substrates conditioned with different activities of Pb^{2+} (Fig. 4B). It shows that the ISM-component modified paper substrates are chemically active in terms of their selective interactions with the analyte (Pb^{2+}). The higher the activity of Pb^{2+} used for conditioning the paper substrates, the higher the absolute potential of the Pb^{2+}-ISEs. This is especially valid for Pb^{2+}-ISE responses utilizing $10^{-1.42}$, $10^{-2.17}$, and $10^{-3.06}$ M Pb^{2+} solutions, where the slopes of the potential increases were obtained from all sensor responses at specific activities of standard solutions, *e.g.* 2.4 ± 2.5 mV dec^{-1} (at $10^{-2.17}$ M Pb^{2+}), 3.5 ± 3.0 mV dec^{-1} (at $10^{-3.06}$ M Pb^{2+}), and 8.2 ± 1.7 mV dec^{-1} (at $10^{-4.02}$ M Pb^{2+}). This shows that ISM is selective towards Pb^{2+} and its conditioning state influences the Pb^{2+}-ISEs responses as different conditioned membrane phases are in direct contact with each other (phase 1: ISM on a paper substrate and phase 2: ISM of ISE). However, considering the performance of the PS6.0 conditioned with different primary ion concentrations in comparison with that of the unconditioned PS6.0, the unconditioned PS6.0 was the best performing paper substrate in terms of controlled potentiometric response, having the best linearity (R^2 = 0.9994) and having a lower uncertainty (standard deviation in EMFs measured at each Pb^{2+} activity).

 This journal is © The Royal Society of Chemistry 2022

Published on 17 August 2022. Downloaded on 28/1/2026 8:06:14 PM.

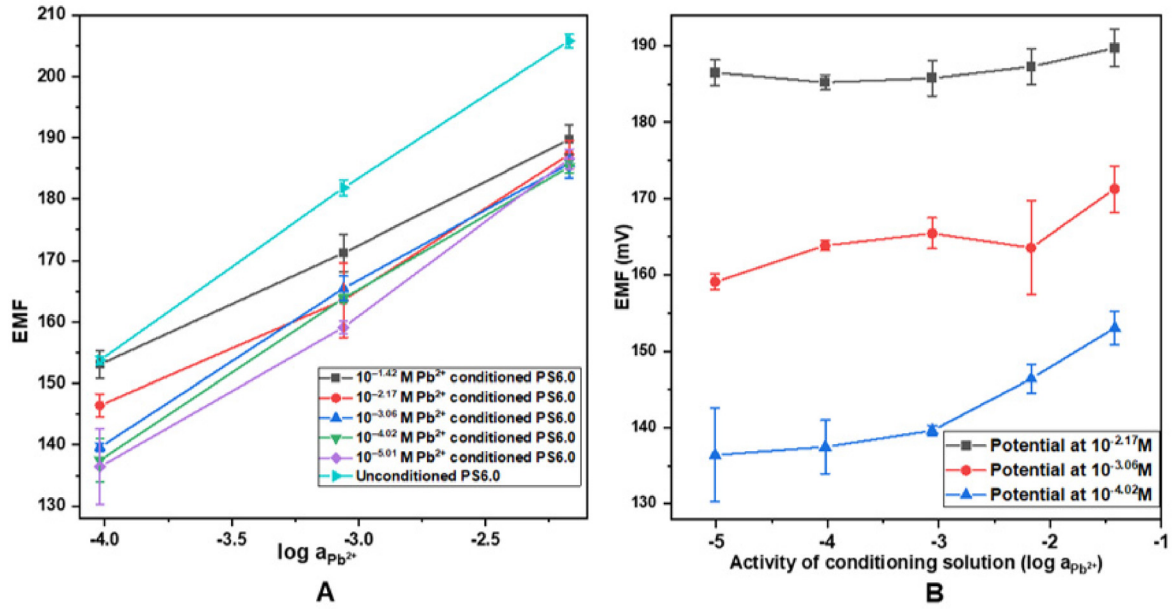

Fig. 4 Potentiometric response of Pb^{2+}-ISEs coupled with PS6.0 treated with different concentrations of Pb^{2+} (A) and variation of EMF at different Pb^{2+} activities for Pb^{2+}-ISEs coupled with ISM component modified paper substrates conditioned with different activities of Pb^{2+} (B).

The effect of conditioning the ISM modified paper substrates with $Cd(NO_3)_2$ (interfering ion) was also studied and the results are shown in Fig. S3.† The Cd^{2+} ion was considered as a model interfering ion in this study as cadmium is one of the major interfering ions for Pb^{2+}-ISEs based on lead ionophore IV with $\log K_{Pb^{2+},Cd^{2+}} = -3.8$.[35] It was found that conditioning of PS6.0 with the interfering ion (Cd^{2+}) did not influence (positively or negatively) the response of the Pb^{2+}-ISEs (having a selectivity coefficient favoring lead(II) over cadmium (II)). It can then be expected that ISM in the structures of the paper substrates maintains the selectivity of the lead ionophore IV-based ISM. The selectivity of the Pb^{2+}-ISE was confirmed using the separate solution method (Table 1). The selectivity coefficients obtained in solution were comparable to or slightly higher than those obtained when Pb^{2+}-ISEs were used with PS6.0 as a sampling substrate. Naturally, the paper matrix may produce additional ionic content, making the selectivity coefficients biased and shifting the selectivity of the Pb^{2+}-ISEs to higher values when used with paper substrates. What is important to note is that the most interfering ions, namely Cu^{2+} and Cd^{2+}, remain at low interference levels validating the performance of the Pb^{2+}-ISM to be predominantly Pb^{2+} selective.

Table 1 Observed selectivity coefficients and slopes obtained using the separate solution method for Pb^{2+}-ISEs in solution and incorporated with ISM-modified paper; the slopes indicated are between $10^{-3.06}$ and $10^{-2.17}$ M of the respective interfering ion

j	$\log K^{pot}_{Pb^{2+},j}$ in solution	Slope/mV dec^{-1} in solution	$\log K^{pot}_{Pb^{2+},j}$ with PS6.0	Slope/mV dec^{-1} with PS6.0
Ca^{2+}	−15.8 ± 0.8	20.1 ± 0.5	−13.8 ± 1.1	26.0 ± 1.5
Co^{2+}	−15.8 ± 0.7	16.8 ± 4.8	−15.3 ± 0.9	13.2 ± 4.6
Na^{+}	−13.5 ± 0.8	13.1 ± 0.7	−10.8 ± 0.4	26.4 ± 1.1
Ba^{2+}	−13.4 ± 0.6	26.3 ± 1.7	−13.4 ± 0.7	34.4 ± 1.3
Zn^{2+}	−11.4 ± 0.6	27.3 ± 0.4	−12.7 ± 0.3	16.2 ± 4.5
K^{+}	−11.0 ± 0.6	51.8 ± 0.4	−10.5 ± 0.6	23.3 ± 5.8
Cu^{2+}	−10.6 ± 0.7	19.2 ± 0.9	−8.6 ± 0.6	37.2 ± 1.1
Cd^{2+}	−5.8 ± 0.3	30.8 ± 1.2	−6.3 ± 0.3	29.5 ± 1.3
Pb^{2+}	0	28.3 ± 0.2	0	27.5 ± 1.8

Characterization of ISM-modified paper substrates

The best performing ISM-modified paper substrates were characterized for their chemical and physical properties that may be influencing the potentiometric response when coupled with Pb^{2+}-ISEs. For example, the liquid absorption capacity gradually decreased from PS6.3 to PS6.0. Similarly, the response time of the Pb^{2+}-ISEs increased from PS6.3 to PS6.0 (Table 2) This can be explained by the fact that membrane components occupy the available space in between and within the cellulose fibres that ultimately limits the wicking ability of the paper. Both liquid absorption capacity and ISE response times assure that all paper modifications are viable for analytical measurements within small liquid volumes and the time of

Table 2 Liquid absorption capacity of the modified paper substrates and response time of the Pb^{2+}-ISEs when coupled with modified paper substrates

PS	Liquid absorption capacity (μL cm^{-2})	Potentiometric measurement response time of Pb^{2+}-ISEs (s)
6.3	38.97 ± 5.31	16.7 ± 4.2
6.2	24.80 ± 4.84	18.7 ± 3.1
6.1	18.88 ± 3.98	20.0 ± 6.9
6.0	17.27 ± 3.27	24.0 ± 4.0

Published on 17 August 2022. Downloaded on 28/1/2026 8:06:14 PM.

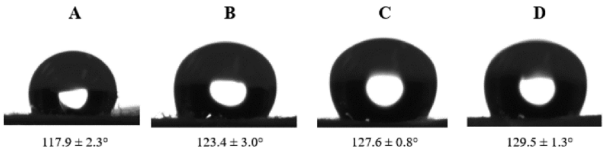

Fig. 5 Contact angle measurements: optical images taken in sessile drop mode for PS6.3 (A), PS6.2 (B), PS6.1 (C) and PS6.0 (D).

measurement is not longer than typically assumed 60 s. Furthermore, as ISM is hydrophobic in nature with the introduction of a higher mass of membrane components to the paper substrate an imminent increase in the hydrophobicity of the modified paper substrates was observed (Fig. 5). Aside from ISM occupying the available space in between and within paper fibres, the increase in the hydrophobicity of the paper substrates could also be a reason for the increase in the Pb^{2+}-ISE response time.

When considering the SEM images of the ISM-modified paper substrates (Fig. S4†), the images of modified paper substrates and unmodified paper substrates at different magnifications did not show much variation in terms of the distribution of the paper fibres and the overall surface morphology.

However, some granular structures could be observed at higher magnifications in modified paper substrates and the concentration of these structures increased with increasing membrane cocktail concentrations (PS6.3 to PS6.0) suggesting that more and more ISM components were distributed throughout the surface of the paper substrates. Fig. S5† shows elemental mapping done with EDX where all ISM modified paper substrates indicate the presence of element chlorine apart from the usual carbon and oxygen present in unmodified paper substrates. The presence of chlorine was from PVC used for the modification of paper substrates (33.3 w/w% in ISM). Interestingly, in PS6.0 sulphur could also be observed in addition to chlorine, carbon and oxygen. The presence of sulphur most likely originated from lead ionophore IV used for modification (1% w/w in ISM). The absence of sulphur in EDX elemental mapping from PS6.1 to 6.3 could be due to the low concentration of the ionophore within the paper substrates and the relatively high detection limit of EDX. In order to investigate whether the extra elements from the paper modification distribute evenly, the individual maps of the elements were also obtained and are shown in Fig. 6 (left). All the elements were distributed throughout the surface of the paper, and the elements originating from the ISM seemed to be found along the edges of the paper fibres. The cross-section of a modified paper substrate was also obtained and EDX was performed. Fig. 6 (right) shows that ISM components were distributed throughout the cross-section of the paper substrate indicating the full bulk of the paper substrate modification.

An FTIR study was performed to provide additional insight into and supporting evidence to the chemical modification of paper substrates by ISM. As shown in Fig. S6 and Table S2,† the FTIR spectra indicated that the modification of the PS6.0 paper substrate demonstrated multiple additional functional groups (as compared to the unmodified paper substrate) that are correlated to the ISM components applied.[41–43] Detailed FTIR analysis is available in ESI section 2.1.†

Determination of lead(II) in complex environmental samples using ISM-modified paper substrates coupled with Pb^{2+}-ISEs

Overall, the Pb^{2+} ion activities determined by the ISEs coupled with ISM-modified paper substrates (PS6.0) were found to be comparable to the total lead concentration determined by ICP-OES (Fig. 7). The uncertainties of most measurements were within ±20% between these two measurements with some slight deviation for the wetland sample, cultivation soil sample and biowaste 1 sample. The higher variations of the

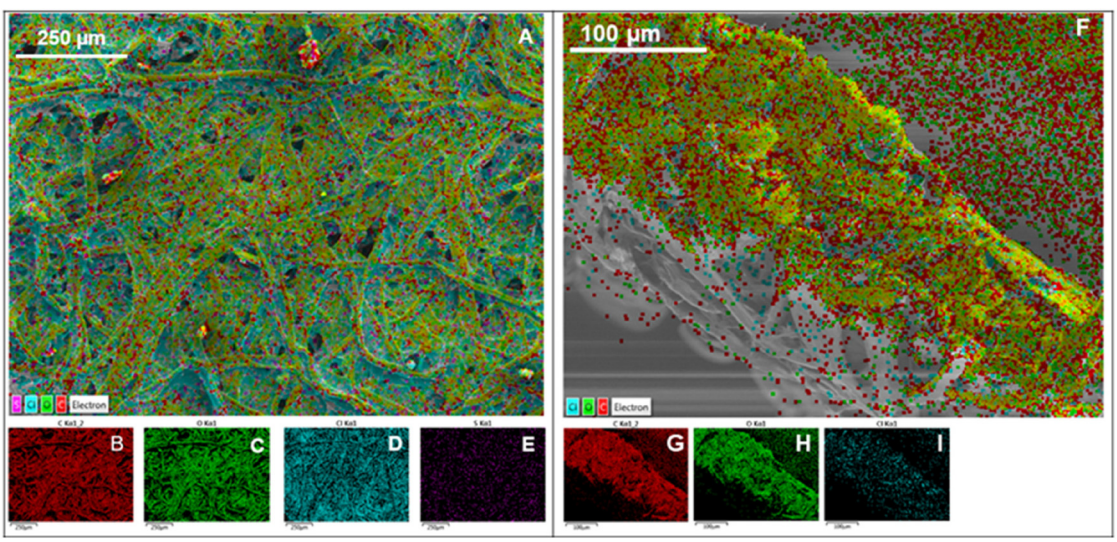

Fig. 6 Elemental mapping of surface (left) and cross-section (right) of PS6.0 where A and F show the overlapped elemental images and B, C, D, E, G, H, and I show the individual element maps of carbon (red), oxygen (green), chlorine (light blue), and sulphur (purple).

 This journal is © The Royal Society of Chemistry 2022

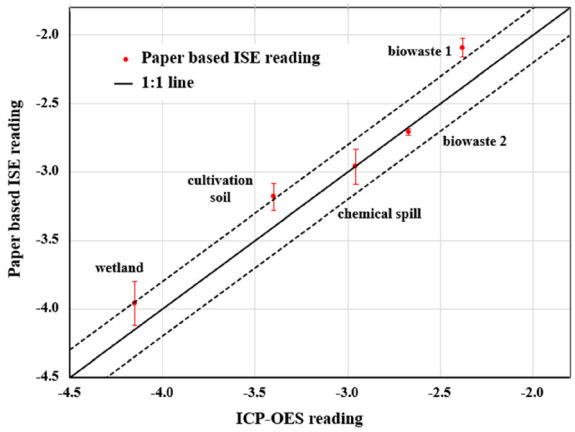

Fig. 7 Determination of lead(II) in samples with complex environmental matrices using ISM-component modified paper substrates coupled with Pb^{2+}-ISEs as compared to the measurement done by ICP-OES.

Published on 17 August 2022. Downloaded on 28/1/2026 8:06:14 PM.

results between potentiometric and ICP-OES measurements, for wetland and cultivation soil samples, could be due to the possible interactions of Pb^{2+} with organic matter that is expected to be present in these types of samples. This would partially deplete the ionized lead(II) from the samples. For biowaste 1, the ionic strength of the leachate could possibly be high enough to shift the calibration and measurement apart inducing measurement errors. Nonetheless, all measurements conducted bring a great promise to use ISM-component modified paper substrates coupled with Pb^{2+}-ISEs for measurement of ion activity in samples containing high solid-to-liquid ratios and complex environmental matrices.

Conclusions

ISM-component modified paper substrates were validated for their use as microfluidic sampling substrates when coupled with Pb^{2+}-ISEs. It was found that direct modification of paper substrates by traditional ISM cocktail used for the preparation of Pb^{2+}-ISEs was the most optimal in (i) eliminating super-Nernstian response of ISEs when unmodified paper substrates were used for solution sampling; (ii) improving the uncertainty of measurements when unconditioned ISM-component modified paper substrates were used; and (iii) extending the linear working range of the sensor to be comparable to standard beaker-based measurements.

Moreover, the use of the same chemicals to prepare ISM of ISE and modify the paper substrates simplifies the procedure of preparation of the measuring setup and may have further direct economic benefits by limiting the preparation of the measuring setup to a limited number of chemicals. Finally, having ISM on paper substrates simplifies the ISM|modified paper substrate interface by being more compatible with the one of ISM. It was found that ISM on paper substrates may influence the potentiometric response of the Pb^{2+}-ISEs used. For that reason, the unconditioned ISM-component modified paper substrates were found to be the best suited for the successful determination of lead(II) in complex environmental samples.

Author contributions

Rochelle Silva: Methodology, investigation, formal analysis, and writing – original draft, Zhao Ke: investigation, Ding Ruiyu: methodology, investigation, and writing – review, Wei Ping Chan: investigation, Mingpeng Yang: investigation, Jane Si Qi Yip: investigation, and Grzegorz Lisak: conceptualization, methodology, resources, writing – review & editing, supervision, funding acquisition, and project administration.

Conflicts of interest

There are no conflicts to declare.

Acknowledgements

Rochelle Silva is a recipient of the NTU Research Scholarship. This research is supported by the National Research Foundation, Singapore, and PUB, Singapore's National Water Agency under its RIE2025 Urban Solutions and Sustainability (USS) (Water) Centre of Excellence (CoE) Programme which provides funding to the Nanyang Environment & Water Research Institute (NEWRI) of the Nanyang Technological University, Singapore (NTU). Any opinions, findings and conclusions or recommendations expressed in this material are those of the author(s) and do not reflect the views of National Research Foundation, Singapore and PUB, Singapore's National Water Agency. We would like to acknowledge Mr She Ka Keng and Mr Tu Wei Han from NEWRI for their guidance with analytical techniques.

References

1 R. D. Johnson and L. G. Bachas, Ionophore-based ion-selective potentiometric and optical sensors, *Anal. Bioanal. Chem.*, 2003, **376**, 328–341.
2 E. Bakker, P. Bühlmann and E. Pretsch, Carrier-Based Ion-Selective Electrodes and Bulk Optodes. 1. General Characteristics, *Chem. Rev.*, 1997, **97**, 3083–3132.
3 A. Ceresa, E. Bakker, B. Hattendorf, D. Günther and E. Pretsch, Potentiometric Polymeric Membrane Electrodes for Measurement of Environmental Samples at Trace Levels: New Requirements for Selectivities and Measuring Protocols, and Comparison with ICPMS, *Anal. Chem.*, 2001, **73**, 343–351.
4 F. Faridbod, P. Norouzi, R. Dinarvand and M. R. Ganjali, Developments in the Field of Conducting and Non-conducting Polymer Based Potentiometric Membrane Sensors for Ions Over the Past Decade, *Sensors*, 2008, **8**, 2331–2412.

Published on 17 August 2022. Downloaded on 28/1/2026 8:06:14 PM.

5 C. Bahro, S. Goswami, S. Gernhart and D. Koley, Calibration-free Solid-State Ion-Selective Electrode Based on a Polarized PEDOT/PEDOT-S-Doped Copolymer as Back Contact, *Anal. Chem.*, 2022, **94**, 8302–8308.
6 C. R. Rousseau and P. Bühlmann, Calibration-free potentiometric sensing with solid-contact ion-selective electrodes, *TrAC, Trends Anal. Chem.*, 2021, **140**, 116277.
7 R. De Marco, G. Clarke and B. Pejcic, Ion-Selective Electrode Potentiometry in Environmental Analysis, *Electroanalysis*, 2007, **19**, 1987–2001.
8 T. Forrest, E. Zdrachek and E. Bakker, Thin Layer Membrane Systems as Rapid Development Tool for Potentiometric Solid Contact Ion-selective Electrodes, *Electroanalysis*, 2020, **32**, 799–804.
9 Y. H. Cheong, L. Ge and G. Lisak, Highly reproducible solid contact ion selective electrodes: Emerging opportunities for potentiometry – A review, *Anal. Chim. Acta*, 2021, **1162**, 338304.
10 R. Wang, X. Du, X. Ma, J. Zhai and X. Xie, Ionophore-based pH independent detection of ions utilizing aggregation-induced effects, *Analyst*, 2020, **145**, 3846–3850.
11 H. Shibata, T. G. Henares, K. Yamada, K. Suzuki and D. Citterio, Implementation of a plasticized PVC-based cation-selective optode system into a paper-based analytical device for colorimetric sodium detection, *Analyst*, 2018, **143**, 678–686.
12 E. Hupa, U. Vanamo and J. Bobacka, Novel Ion-to-Electron Transduction Principle for Solid-Contact ISEs, *Electroanalysis*, 2015, **27**, 591–594.
13 Z. Jarolímová, T. Han, U. Mattinen, J. Bobacka and E. Bakker, Capacitive Model for Coulometric Readout of Ion-Selective Electrodes, *Anal. Chem.*, 2018, **90**, 8700–8707.
14 J. Zhai, D. Yuan and X. Xie, Ionophore-based ion-selective electrodes: signal transduction and amplification from potentiometry, *Sens. Diagn.*, 2022, **1**, 213–221.
15 V. Krikstolaityte, R. Ding, E. Chua Hui Xia and G. Lisak, Paper as sampling substrates and all-integrating platforms in potentiometric ion determination, *TrAC, Trends Anal. Chem.*, 2020, **133**, 116070.
16 A. K. Yetisen, M. S. Akram and C. R. Lowe, Paper-based microfluidic point-of-care diagnostic devices, *Lab Chip*, 2013, **13**, 2210–2251.
17 W. Mazurkiewicz, M. Podrażka, E. Jarosińska, K. Kappalakandy Valapil, M. Wiloch, M. Jönsson-Niedziółka and E. Witkowska Nery, Paper-Based Electrochemical Sensors and How to Make Them (Work), *ChemElectroChem*, 2020, **7**, 2939–2956.
18 A. T. K. Perera, D.-T. Phan, S. Pudasaini, Y. Liu and C. Yang, Enhanced sample pre-concentration by ion concentration polarization on a paraffin coated converging microfluidic paper based analytical platform, *Biomicrofluidics*, 2020, **14**, 014103.
19 R. Ding, N. K. Joon, A. Ahamed, A. Shafaat, M. Guzinski, M. Wagner, T. Ruzgas, J. Bobacka and G. Lisak, Gold-modified paper as microfluidic substrates with reduced biofouling in potentiometric ion sensing, *Sens. Actuators, B*, 2021, **344**, 130200.
20 R. Ding, M. Fiedoruk-Pogrebniak, M. Pokrzywnicka, R. Koncki, J. Bobacka and G. Lisak, Solid reference electrode integrated with paper-based microfluidics for potentiometric ion sensing, *Sens. Actuators, B*, 2020, **323**, 128680.
21 R. Ding, Y. H. Cheong, A. Ahamed and G. Lisak, Heavy Metals Detection with Paper-Based Electrochemical Sensors, *Anal. Chem.*, 2021, **93**, 1880–1888.
22 G. Lisak, Reliable environmental trace heavy metal analysis with potentiometric ion sensors - reality or a distant dream, *Environ. Pollut.*, 2021, **289**, 117882.
23 G. Lisak, J. Cui and J. Bobacka, Paper-based microfluidic sampling for potentiometric determination of ions, *Sens. Actuators, B*, 2015, **207**, 933–939.
24 R. Ding, V. Krikstolaityte and G. Lisak, Inorganic salt modified paper substrates utilized in paper based microfluidic sampling for potentiometric determination of heavy metals, *Sens. Actuators, B*, 2019, **290**, 347–356.
25 R. Ding, Y. H. Cheong, K. Zhao and G. Lisak, Acidified paper substrates for microfluidic solution sampling integrated with potentiometric sensors for determination of heavy metals, *Sens. Actuators, B*, 2021, 130567.
26 R. Silva, A. Ahamed, Y. H. Cheong, K. Zhao, R. Ding and G. Lisak, Non-equilibrium potentiometric sensors integrated with metal modified paper-based microfluidic solution sampling substrates for determination of heavy metals in complex environmental samples, *Anal. Chim. Acta*, 2022, **1197**, 339495.
27 U. Schaller, E. Bakker, U. E. Spichiger and E. Pretsch, Ionic additives for ion-selective electrodes based on electrically charged carriers, **https://pubs.acs.org/doi/pdf/10.1021/ac00075a013**, (accessed 26 January 2022).
28 E. M. Zahran, A. New, V. Gavalas and L. G. Bachas, Polymeric plasticizer extends the lifetime of PVC-membrane ion-selective electrodes, *Analyst*, 2014, **139**, 757–763.
29 J. D. R. Thomas, Solvent polymeric membrane ion-selective electrodes, *Anal. Chim. Acta*, 1986, **180**, 289–297.
30 K. N. Mikhelson, in *Ion-Selective Electrodes*, ed. K. N. Mikhelson, Springer, Berlin, Heidelberg, 2013, pp. 51–95.
31 K. N. Mikhelson, in *Ion-Selective Electrodes*, ed. K. N. Mikhelson, Springer, Berlin, Heidelberg, 2013, pp. 11–32.
32 J. Bobacka, Potential Stability of All-Solid-State Ion-Selective Electrodes Using Conducting Polymers as Ion-to-Electron Transducers, *Anal. Chem.*, 1999, **71**, 4932–4937.
33 P. C. Meier, Two-parameter debye-hückel approximation for the evaluation of mean activity coefficients of 109 electrolytes, *Anal. Chim. Acta*, 1982, **136**, 363–368.
34 N. K. Joon, J. E. Barnsley, R. Ding, S. Lee, R.-M. Latonen, J. Bobacka, K. C. Gordon, T. Ogawa and G. Lisak, Silver(I)-selective electrodes based on rare earth element double-decker porphyrins, *Sens. Actuators, B*, 2020, **305**, 127311.
35 E. Malinowska, Z. Brzózka, K. Kasiura, R. J. M. Egberink and D. N. Reinhoudt, Lead selective electrodes based on thioamide functionalized calix[4]arenes as ionophores, *Anal. Chim. Acta*, 1994, **298**, 253–258.

This journal is © The Royal Society of Chemistry 2022

36 A. Ceresa and E. Pretsch, Determination of formal complex formation constants of various Pb2+ ionophores in the sensor membrane phase, *Anal. Chim. Acta*, 1999, **395**, 41–52.
37 F. Pan, Y. Yu, L. Yu, H. Lin, Y. Wang, L. Zhang, D. Pan and R. Zhu, Quantitative assessment on soil concentration of heavy metal–contaminated soil with various sample pretreatment techniques and detection methods, *Environ. Monit. Assess.*, 2020, **192**, 800.
38 N. Ruecha, O. Chailapakul, K. Suzuki and D. Citterio, Fully Inkjet-Printed Paper-Based Potentiometric Ion-Sensing Devices, *Anal. Chem.*, 2017, **89**, 10608–10616.
39 M. Novell, M. Parrilla, G. A. Crespo, F. X. Rius and F. J. Andrade, Paper-Based Ion-Selective Potentiometric Sensors, *Anal. Chem.*, 2012, **84**, 4695–4702.
40 J. Hu, A. Stein and P. Bühlmann, A Disposable Planar Paper-Based Potentiometric Ion-Sensing Platform, *Angew. Chem., Int. Ed.*, 2016, **55**, 7544–7547.
41 J. Coates, in *Encyclopedia of Analytical Chemistry*, John Wiley & Sons, Ltd, 2006.
42 J. Chen, X. A. Nie, J. C. Jiang and Y. H. Zhou, Thermal degradation and plasticizing mechanism of poly(vinyl chloride) plasticized with a novel cardanol derived plasticizer, *IOP Conf. Ser.: Mater. Sci. Eng.*, 2018, **292**, 012008.
43 A. Mancilla-Rico, J. de Gyves and E. Rodríguez de San Miguel, Structural Characterization of the Plasticizers' Role in Polymer Inclusion Membranes Used for Indium(III) Transport Containing IONQUEST® 801 as Carrier, *Membranes*, 2021, **11**, 401.

Published on 17 August 2022. Downloaded on 28/1/2026 8:06:14 PM.